DEUTSCHES ELEKTRONEN – SYNCHROTRON DESY

DESY SR 89-03
July 1989

NIKOS II - A System for Non-Invasive Imaging of Coronary Arteries

W.-R. Dix, K. Engelke, G. Heintze, J. Heuer, W. Graeff
Hamburger Synchrotronstrahlungslabor HASYLAB at DESY, Hamburg

W. Kupper
Kardiologische Abteilung der Medizinischen Klinik, Universitäts-Krankenhaus Eppendorf, Hamburg

M. Lohmann, K.-H. Stellmaschek
Institut für Mathematik und Datenverarbeitung in der Medizin, Universitäts-Krankenhaus Eppendorf, Hamburg

I. Makin
Fachhochschule Hamburg, Hamburg.

T. Möchel, R. Reumann
II. Institut für Experimentalphysik, Universität Hamburg

ISSN 0723-7979

NOTKESTRASSE 85 · 2 HAMBURG 52

To be sure that your preprints are promptly included in the
HIGH ENERGY PHYSICS INDEX,
send them to the following address (if possible by air mail):

DESY
Bibliothek
Notkestrasse 85
2 Hamburg 52
Germany

DESY SR 89-03
July 1989

ISSN 0723-7979

NIKOS II - a system for non-invasive imaging of coronary arteries.

W.-R. Dix[a], K. Engelke[a], G. Heintze[a], J. Heuer[a], W. Graeff[a], W. Kupper[b], M. Lohmann[c], I. Makin[d], T. Möchel[e], R. Reumann[e], K.-H. Stellmaschek[c]

[a]Hamburger Synchrotronstrahlungslabor HASYLAB at DESY, 2000 Hamburg 52, FRG
[b]Kardiologische Abt. der Medizinischen Klinik, Universitäts-Krankenhaus Eppendorf, 2000 Hamburg 20, FRG
[c]Inst. für Mathematik und Datenverarbeitung in der Medizin, Universitäts-Krankenhaus Eppendorf, 2000 Hamburg 20, FRG
[d]Fachhochschule Hamburg, 2050 Hamburg 80, FRG
[e]II. Inst. für Experimentalphysik, Universität Hamburg, 2000 Hamburg 36, FRG

ABSTRACT

This paper presents results of the initial in-vivo investigations with the system NIKOS II (NIKOS = Nicht-invasive Koronarangiographie mit Synchrotronstrahlung), an advanced version of NIKOS I which was developed since 1981. Aim of the work is to be able to visualize coronary arteries down to $1mm$ diameter with an iodine mass density of $1mg/cm^2$, thus allowing non-invasive investigations by intravenous injection of the contrast agent. For this purpose Digital Subtraction Angiography (DSA) in energy subtraction mode (dichromography) is employed. The two images for subtraction are taken at photon energies just below and above the iodine K-edge ($33.17keV$). After subtraction the background contrast from bone and soft tissue is suppressed and the iodinated structures are strongly enhanced because of the abrupt change of absorption at the K-edge. The two monoenergetic beams are filtered out of a synchrotron radiation beam by a crystal monochromator and measured with a two line detector. One scan (two images) lasts between $250ms$ (final version) and $1s$ (at present). The images from the in-vivo investigations of dogs have been promising. The right coronary artery (diameter $1.5mm$) was clearly visible. With application of better image processing algorithms the images illustrated in this paper have a definite potential for improvement.

to be published in: SPIE Vol. 1090
Medical Imaging III:
Image Formation

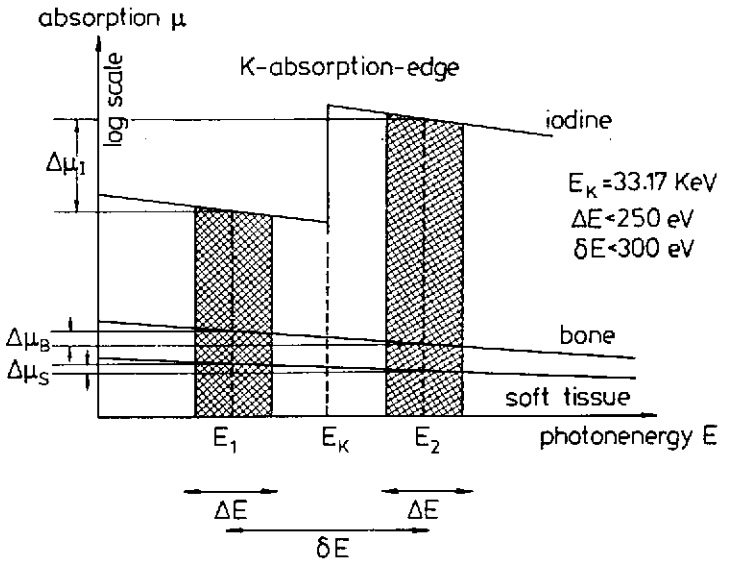

Figure 1: K-edge of iodine at $E_K = 33.17keV$. E_1 and E_2 denote the two energies of the quasi-monoenergetic beams for dichromography with bandwidth ΔE.

1. INTRODUCTION

Myocardial infarction is one of the leading causes of death in the industrialised world. The reason for an acute myocardial infarction being predominantly an acute thrombotic occlusion of a coronary artery at the site of a pre-existent stenosis, it is of considerable interest to identify stenoses in the coronary arteries before the incidence of an acute myocardial infarction. At present, the only method to view stenoses in coronary arteries is invasive coronary angiography where a catheter is inserted via the arterial system up to the ostia of the coronary arteries. The resulting images are of high quality but the concomitant risk involved with the method considerably offsets the advantages. The considerably high morbidity and mortality rates associated with invasive angiography being 1.2 to 2.2% and 0.07 to 0.23% quite positively justify efforts to develop a non-invasive method without catheterisation for the visualisation of coronary arterial stenoses.

If the contrast medium is introduced into the brachial vein, it would be diluted by a factor of about 40 by the time it enters the coronary arteries. Assuming injection of a bolus of $10ml$ of the commercially available radiopaque iodine with concentration of $370mg/ml$ as contrast medium within $1s$, the concentration in the coronary arteries would be $10mg/ml$ of iodine, corresponding to a mass density of $1mg/cm^2$ in a coronary artery of $1mm$ diameter. Imaging of mass densities of this order is not possible by classical X-ray techniques. DSA in time subtraction mode used routinely today for non-invasive investigations cannot be applied because of the rapid pulsation of the heart. Furthermore ECG-triggered imaging of structures of $1mm$ diameter is not possible because of the nonperiodic motion of the heart.

Therefore, efforts have been made recently to use DSA in energy subtraction mode (dichromography) for imaging of coronary arteries[1-3]. The two images for subtraction are taken simultaneously at photon energies just below (E_1) and above (E_2) the iodine K-edge ($33.17keV$), when the contrast medium is present in the coronary arteries (see Fig.1). After subtraction the background contrast like bone and soft tissue is suppressed and the iodinated structures

are strongly enhanced because of the abrupt change of absorption at the K-edge. At present the two monoenergetic beams with high intensity, vital for the method, are only available if synchrotron radiation is used.

The conditions which a dichromography system for the imaging of coronary arteries must fulfil are described in chapter 2. The NIKOS system is based on these parameters. Details of its components are described in chapter 3. With the second version of the system (NIKOS II) in-vivo investigations of dogs were performed. A typical result is shown in chapter 4. The remaining problems, which have to be solved before human patients can be investigated, are discussed in chapter 5.

2. PARAMETERS FOR NIKOS

NIKOS II was optimized on the basis of parameters specified in this section. They were determined by either measurements, calculations and/or simulations. Details can be found in ref.4.

Contrast medium: In clinical practice iodine is normally used as a radiopaque dye. Its K-edge lies at $33.17keV$. As photons of this energy have an absorption length of only $2.1cm$ in soft tissue, one might consider contrast agents with K-edges at higher energies in order to minimize the radiation dose for the patients. Assuming the same concentration as for iodine ($370mg/ml$), the radiation dose could be decreased by using of e.g. Gadolinium (K-edge at $50keV$) as a contrast medium. However, Gadolinium contrast medium is only available up to a concentration of $160mg/ml$. Therefore it is superior to iodine only for soft tissue thicknesses of $25cm$ and above. Hence, at present, iodine appears to be the best suited contrast medium for dichromography.

Mass density: Because state of the art surgery is limited to the operation of coronary arteries thicker than $1mm$ diameter, only arteries down to this diameter have to be clearly visible in the angiograms. Assuming the concentration of iodine mentioned in chapter 1, mass densities of iodine down to $1mg/cm^2$ must be detected. The mass absorption coefficient for iodine is $6.55cm^2/g$ (E_1) and $35.9cm^2/g$ (E_2), respectively. This has to be compared to $0.65cm^2/g$ for bone (ribs) and $0.33cm^2/g$ for soft tissue.

Spatial resolution: In order to image arteries of $1mm$ diameter a spatial resolution of $(0.5mm)^{-1}$ is necessary. This is sufficient to see stenoses of interest (70% and more) in the coronary arteries. Note that a linear improvement of the spatial resolution can only be achieved by a quadratic increase of the radiation dose for the patient.

Dynamic range: Given a signal-to-noise-ratio (SNR) in the subtracted image of at least 3, the minimum dynamic range D of the detector can be calculated. Assuming a ratio of about 60 for the transmission through areas dominated by lung tissue and bone tissue, the dynamic range must typically be $D = 8000$.

Line scan system: Area detectors like image converter/TV-systems are not suited for dichromography mainly due to the high scatter fraction which can amount to 90% in the neighbourhood of lung tissue[5]. Therefore line scan detectors are preferable although they are much slower. In line scan systems the scatter fraction is reduced to about 1.5%. In order to avoid fast moving mechanics in the system, in NIKOS a two line detector is used which

simultaneously records the two lines with different energies. It further has the advantage of making better use of the photon flux than a one line detector with dead times during switching.

Time resolution: The two images have to be taken within one heart cycle. During one heart cycle there are two slow motion phases at the end of systole and diastole with a duration of about $250ms$ each und two fast motion phases of about the same duration. In the RAO-30°-projection for example the distal right coronary artery moves up to $2cm/s$ in the slow motion phase and up to $6cm/s$ in the fast motion phase. Simulations show that the images have to be taken in the slow motion phase to avoid artifacts due to the line scan system. Assuming a heart size of $12.5cm$, the spatial resolution mentioned above and a duration of the slow motion phase of $250ms$ the exposure time per line must not exceed $1ms$. With a pixel size of $0.5 \times 0.5mm^2$ and an allowed shift of the structure of interest in either image of 15% of the pixel size, the time delay between the exposure of the corresponding pixel in the two energy images must not exceed $4ms$ during the slow motion phase.

Energy bandwidth: From the energy separation δE (see Fig.1) the difference in the absorption coefficients $\Delta\mu$ of the different materials can be calculated. For iodine it is about four orders of magnitude higher than those of bone and soft tissue. On the other hand the mass density of bone and soft tissue is much higher than that of iodine. It can be shown that for $\delta E = 300eV$ the soft tissue and bone contrast exceeds the contrast of the smallest iodine structures. Therefore $\delta E = 300eV$ should be the upper limit, resulting in a maximum bandwidth ΔE of $250eV$.

Photon flux: Assuming a minimum SNR of 3 for a $1mm$ thick vessel with an iodine mass density of $1mg/cm^2$, the quantum noise must not exceed 1% in the subtracted image, i.e. 0.7% in the two energy images. Given the spatial and temporal resolution above, an intensity in the monochromatic beam of $10^{11} photons/(mm^2 \cdot s)$ is needed.

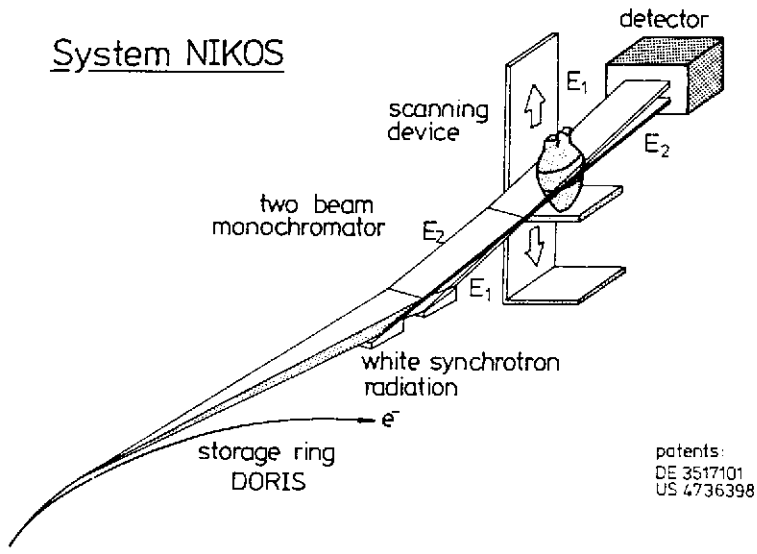

Figure 2: Schematic diagram of NIKOS II. This version of the system was employed for the in-vivo investigations of dogs by the end of 1988.

3. COMPONENTS OF THE SYSTEM

The system NIKOS consists of 6 main components (see Fig.2):
- A hard X-ray wiggler (HARWI) as the synchrotron radiation source,
- a two beam monochromator, which filters the quasi-monoenergetic beams out of the white synchrotron radiation beam,
- a scanning device, which moves the objects through the two monoenergetic beams,
- a two line detector for registration of the two beams,
- a computer system for experiment control, data acquisition, data storage and image processing,
- a safety system for the investigations of patients.

The safety system is not yet installed and is still being developed and tested. The other five components exist in different versions. Their prototypes were tested in the system NIKOS I on a different synchrotron radiation beamline at the storage ring DORIS. They are replaced step by step by improved versions. The stage of development of NIKOS II used at the end of 1988 for in-vivo investigations of dogs, is described in the following subsections as well as the implications for the final system.

3.1. Wiggler HARWI

The wiggler HARWI[6] is installed in the storage ring DORIS at DESY in Hamburg. It fulfils the special needs of dichromography, i.e. a broad beam and high flux at $33.17keV$. The wiggler consists of 20 poles, its total length is $2.4m + 0.12m$ for the endpoles. At present the magnetic gap is $42mm$ high and the maximum field strength is $1.0T$. The horizontal opening angle of the radiation is $6.4mrad$ or $4.4mrad$, respectively, depending on the energy of DORIS. The vertical source size (FWHM) is $1mm$. Behind filters in the beam line ($3mm$ Be, $0.4mm$ C and $1mm$ Al) the power was measured to be $140W$ at $3.68GeV$ electron energy and $80mA$ current at the entrance of the monochromator for a horizontal beam width of $3.5cm$, vertically integrated.

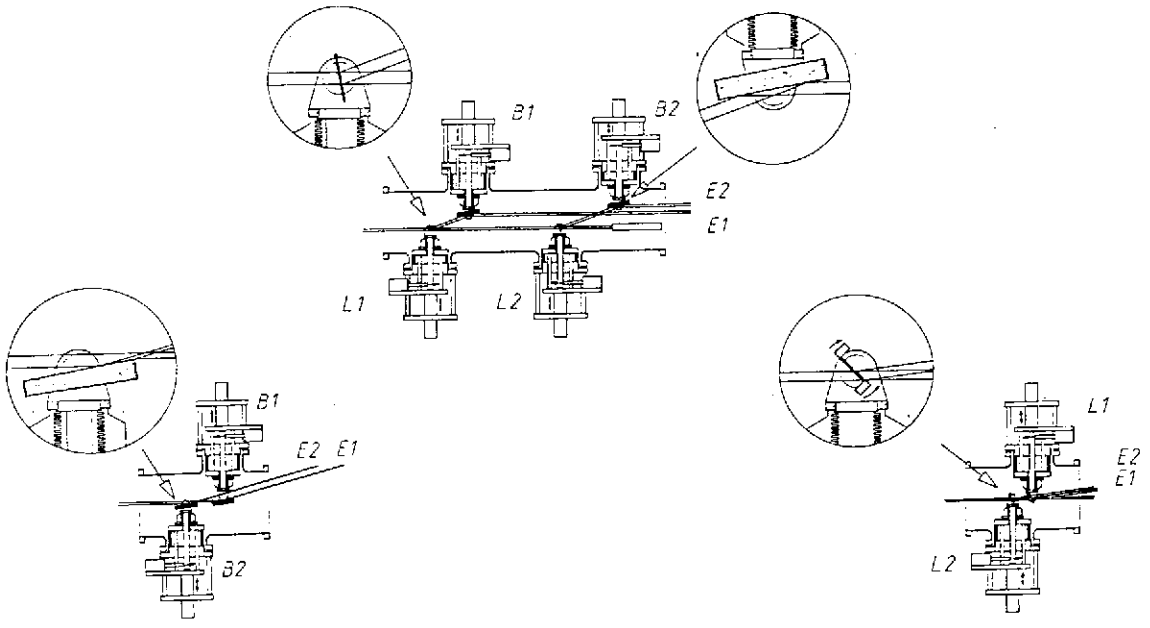

Figure 3: Three versions of the monochromator: (a) Two Laue/Bragg combinations are installed for the two monochromatic beams. (b) Two asymmetric Bragg crystals split the incident white synchrotron radiation beam vertically into two components and reflect the two monochromatic beams. (c) Two successive bent Laue crystals reflect the two monochromatic beams.

A variable vacuum chamber for the wiggler is under development. It will allow a gap height of $30mm$, thus increasing the field to $1.26T$ and doubling the intensity of $33keV$ photons.

3.2. Two beam monochromator

The required beam cross section at the patient is $120 \times 0.5mm^2$. An efficient use of the synchrotron radiation beam requires vertical focussing. Several designs of the monochromator are possible for this purpose[7] (see Fig.3). In all versions single crystals are used for the filtering of the quasi-monochromatic beams out of the white synchrotron radiation beam. Following the Bragg formula $n \cdot \lambda = 2 \cdot d \cdot sin\Theta$ (d = lattice plane spacing in the crystal) in Ge(111) crystals at $\Theta = 3.22°$ (in case of Si(111) crystals $\Theta = 3.42°$) photons of $33.17keV$ are reflected. If the netplanes are oriented perpendicular to the surface the reflected beam leaves the crystal from the reverse side (Laue case) whereas in the Bragg case with netplanes parallel to the surface the beam is reflected from the entrance face. The crystals are mounted in a He-filled tube. They are cooled by gas (Laue crystals) and water (Bragg crystals), respectively.

An optimal design for the monochromator is given by a Laue/Bragg combination for each quasi-monochromatic beam (Fig.3a). We installed two Laue crystals (Si(111)) of $30\mu m$ thickness (optimum for reflectivity at $33.17keV$) and two asymmetric cut Bragg crystals (Ge(111)). The advantages of this design are: higher orders like $99keV$ photons can be rejected by a small detuning of the second crystal ($66keV$ is "not allowed" for (111)-reflections!). As the two beams behind the monochromator only rise slightly (0.14°) due to the combination of Si- and Ge-crystals, the monochromator can be installed halfway between wiggler and patient thus allowing crystals of only $6cm$ width. On the other hand the small rise of the beams allows the shielding of the high energy particles in front of the patient. Furthermore there are no difficulties in the subtraction of bone structures because the two quasi-monochromatic beams

practically do not differ in angle. The thin Laue crystals absorb only a few percent of the total heat load of the white beam and inherently focus the beam without bending the crystal.

A monochromator with two Laue/Bragg combinations was constructed and tested. It was shown to have worked well for a beam width at the object of up to $1cm$. Broader beams showed major horizontal discontinuities in the intensity because of the quality of the Ge crystals employed. At present, crystals of better quality (perfect to a fraction of a second of arc) are not available. Therefore the existing two beam double crystal monochromator cannot be used for routine investigations, yet.

Hence, for the in-vivo investigations of dogs a different design of the monochromator was realized (Fig.3b). Only one crystal is installed for each monochromatic beam, leading to a rise of these beams of about 6.8^o behind the monochromator. In the existing version of the monochromator two $6cm$ wide Ge(111) crystals (Bragg case) are used. Due to the rise of the beam the monochromator must be installed only $3.5m$ in front of the object. Therefore the beam width at the object is only $6cm$. With this monochromator $7 \cdot 10^9 photons/(mm^2 \cdot s)$ were registered in front of the dogs (at $81mA$ current in DORIS). The monochromator needs careful adjustment because small vertical motions of the incident white synchrotron radiation beam result in large changes in the intensity of the two monochromatic beams.

This problem can be overcome by replacing the two crystals (Bragg case) by two bent crystals (Laue case), following an idea of Suortti and Thomlinson[8] (Fig.3c). With this design the intensity of the monochromatic beams could be increased by a factor of 10. The bandwidth of the beams is $\Delta E = 250eV$, depending on the vertical aperture. Such a monochromator with $12cm$ broad Si(111) crystals is being built.

3.3. Scanning device

The scanning device can move loads of up to $300kg$ over a distance of $20cm$ (= 400 lines) with constant speed up to $50cm/s$ (precision 1%). Additional $10cm$ are necessary at either end for acceleration and deceleration. A precise optical scale is mounted on the device. It triggers the readout of the detector every $0.5mm$ (precision $5\mu m$).

Currently a cradle for the investigation of dogs is fixed on the scanning device. For the investigations of patients a special chair has been designed which would allow for rotation around vertical and lateral axes in order to set appropriate projection angles.

3.4. Two line detector

The two line detector (see Fig.4) is based on commercially available photodiode arrays (Reticon RL 1024 SF) which integrate the light generated in a phosphorous layer and amplified by an image intensifier (Proxitronic Proxifier). These three components are coupled via two special fiber optics. In the system NIKOS I a detector with these components was tested[9]. It was suited for two beams of $6cm$ width at a vertical displacement of $2mm$. The electronics allowed a readout of these two lines within $2ms$.

The components of the detector are replaced step by step in order to attain the final version for $12cm$ beam width and $1ms$ readout time. Every new set-up is tested and compared with the previous one.

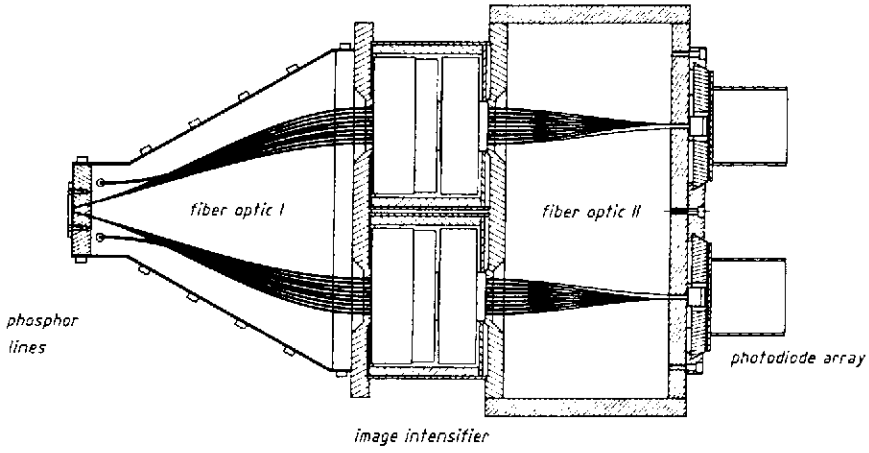

Figure 4: Vertical cut through the NIKOS detector (final version).

The two phosphorous lines at the entrance consist of $Gd_2O_2S : Tb$ powder, sprayed onto a thin lucite plate. They are separated by a reflecting wall. Single crystal scintillators like $CaF_2 : Eu$ or $CdWO_4$ are also being tested. Compared to powder scintillators they have practically no afterglow but their conversion efficiency is less by a factor of 5 to 10.

The light emitted by the scintillators enters a special fiber optics which couples the input line to the entrance face of an image intensifier. Each pixel ($0.5 \times 0.5mm^2$) is connected to a fiber bundle consisting of 25 single glass fibers. The fiber optics rearranges the geometrical figure of the straight input line to a hexagonal pattern at the entrance face of the image intensifier. The fiber optics I and II of the system NIKOS I were also employed for the present investigations. They allow the coupling of two $6cm$ wide lines via one image intensifier to one photodiode array. The numerical aperture of the fiber is 0.59. The new glass fiber optics under development allows the connection of two $12.5cm$ wide lines (250 pixels each) via two image intensifiers to two photodiode arrays. The numerical aperture of the new fiber is 0.87.

The image intensifier is needed to adjust the maximum light output to the saturation level of the photodiodes for an optimal use of the dynamic range of the photodiode arrays. The two-stages intensifier of NIKOS I is replaced by two three-stages devices with fast decay time of the internal phosphors. The overall gain of the new intensifiers was measured to about $200W/W$ in contrast to the specification of the manufacturer of $3000W/W$.

The second fiber optics transforms each pixel from a quadratic cross section of $0.5 \times 0.5mm^2$ to a rectangular shape of $0.1 \times 2.5mm^2$, thus covering exactly the area of four photodiodes of the photodiode array. It is positioned with respect to the photodiodes in such a way that the border between two adjacent fiber bundles falls onto the center of a diode. The output of three diodes is summed up as a pixel signal and the fourth diode signal on the border is discarded.

Based on the experience with NIKOS I, the readout electronics has been completely redesigned. The content of two diodes is now read in parallel. The generated analog signals are amplified and converted in two ADCs (Datel 505 with 12 bit resolution, readout time $500ns$). The digitized signals of three diodes are summed up and stored in a fast buffer. Hence the full scale of the output signal of one pixel is represented by theoretically 12285 grey levels. The two photodiode arrays (each corresponding to one line) are read in parallel within $1.02ms$. Tests showed that the electronics saturates at 10000 grey levels and that an offset of about

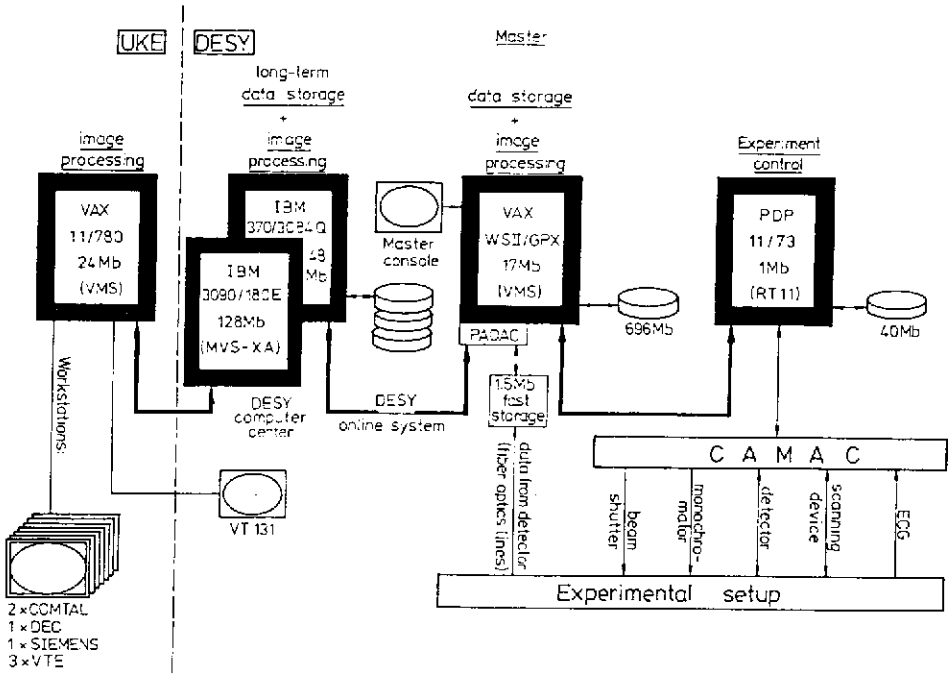

Figure 5: The main parts of the NIKOS computer system

600 grey levels exists. The afterglow differs very much in the readout of different photodiode arrays but was less in comparison to NIKOS I by about 0.5% for the best out of 5 photodiode arrays. At large grey levels a crosstalk from pixel to pixel arises. All these facts decrease the dynamic range of the detector and should be overcome by small changes in the layout of the different circuits. With the existing set-up a preliminary determination of the dynamic range gives $D = 3000$.

3.5. Computer system

At the experimental site two computers are installed:
• A VAX-WSII/GPX for the coordination of the computer system, for data acquisition, image processing and presentation serves as a master.
• A PDP 11/73 is connected to the first machine via a serial line. The machine is used for the control of the complete experimental set-up, i.e. monchromator, detector, scanning device, ECG, beam shutter.

The two machines are connected via the DESY online-system (PADAC - in-house system of DESY with a transfer rate of $200 kbyte/s$) to the DESY computer center.

The incoming data are transfered from the detector via a glass fiber link to a fast storage at the VAX-WSII/GPX with a rate of $4 \cdot 10^6 baud$. Two such links work in parallel for the two energy images. Up to 4 scans (2 images with 256 × 256 pixels, each) can be stored at a time.

Image processing can be done on three different computers:
• Relatively simple processing during the investigations on the master computer at the experimental site,

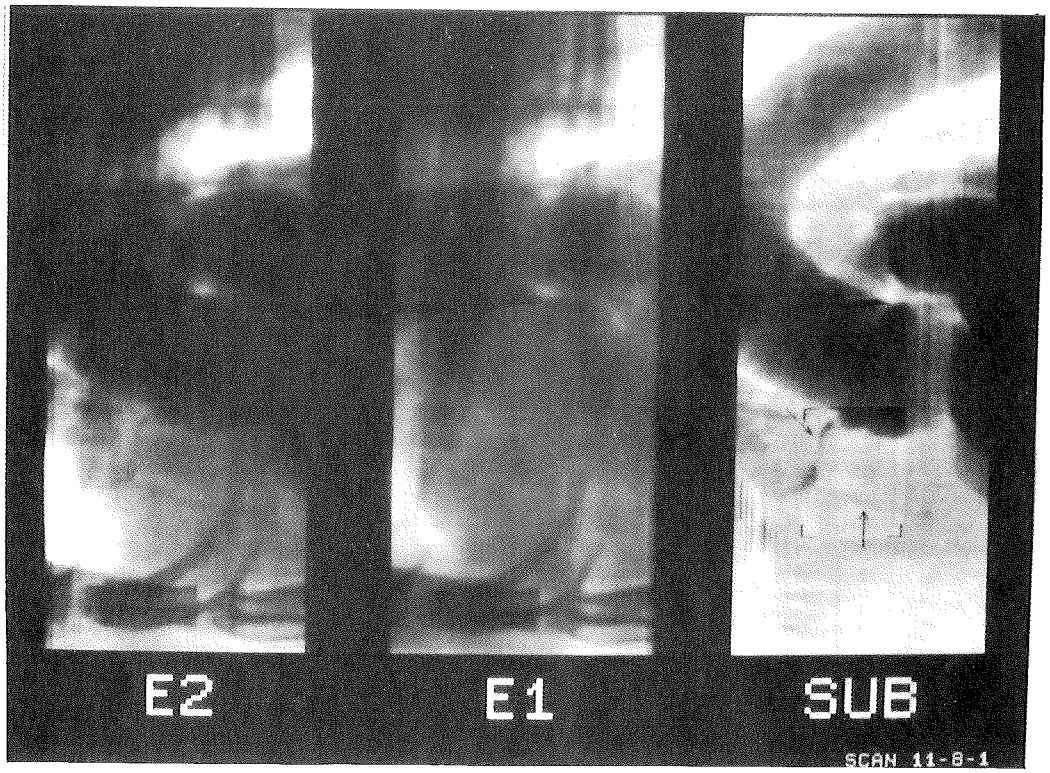

Figure 6: Two energy images (6a, 6b) and subtraction image (6c) of an in-vivo investigation of a dog. In the subtraction image parts of the aorta and of the left chambers are visible. The arrows mark the right coronary artery (for details see text).

- time consuming processing at the DESY computer center,
- specialized processing on the computer of the Dept. of Computer Science in Medicine.

4. IN-VIVO INVESTIGATIONS

With the system NIKOS II as described above three dogs were investigated. Their weight was $11kg$ to $23kg$, the width of the ribcage being $13cm$ to $18cm$. The dogs were anaesthetized for about four hours.

Fig.6 illustrates the resulting images. In this case the weight of the dog was $23kg$, the chest to be penetrated was $18cm$. The dog was placed in abdominal position. The pulse rate fluctuated between $30/min$ and $60/min$. A 5f-catheter was positioned in the vena cava superior. $10ml$ of contrast medium (Ultravist-370 with $370mg/ml$ of iodine) were injected within $2s$ via the catheter. This resulted in $11mg/ml$ of iodine in the aorta and $1.6mg/cm^2$ in the right coronary artery of $1.5mm$ diameter. The scan was started ECG-triggered $17.5s$ after injection of the contrast medium with a speed of $12.5cm/s$. The scan (244 lines) was completed within $975ms$. The current in the storage ring was $70mA$, the energy $3.68GeV$. The measurement of the skin dose gave $0.8rem/scan$.

The raw data are processed in the following way:
- The dark current of the detector is subtracted.
- The single lines are corrected for instabilities in the motion of the scanning device. During the scan the individual exposure time has been determined using a fast clock.
- The two energy images are separated as they are mixed in the raw data due to the special form of the fiber optics in the detector[9].

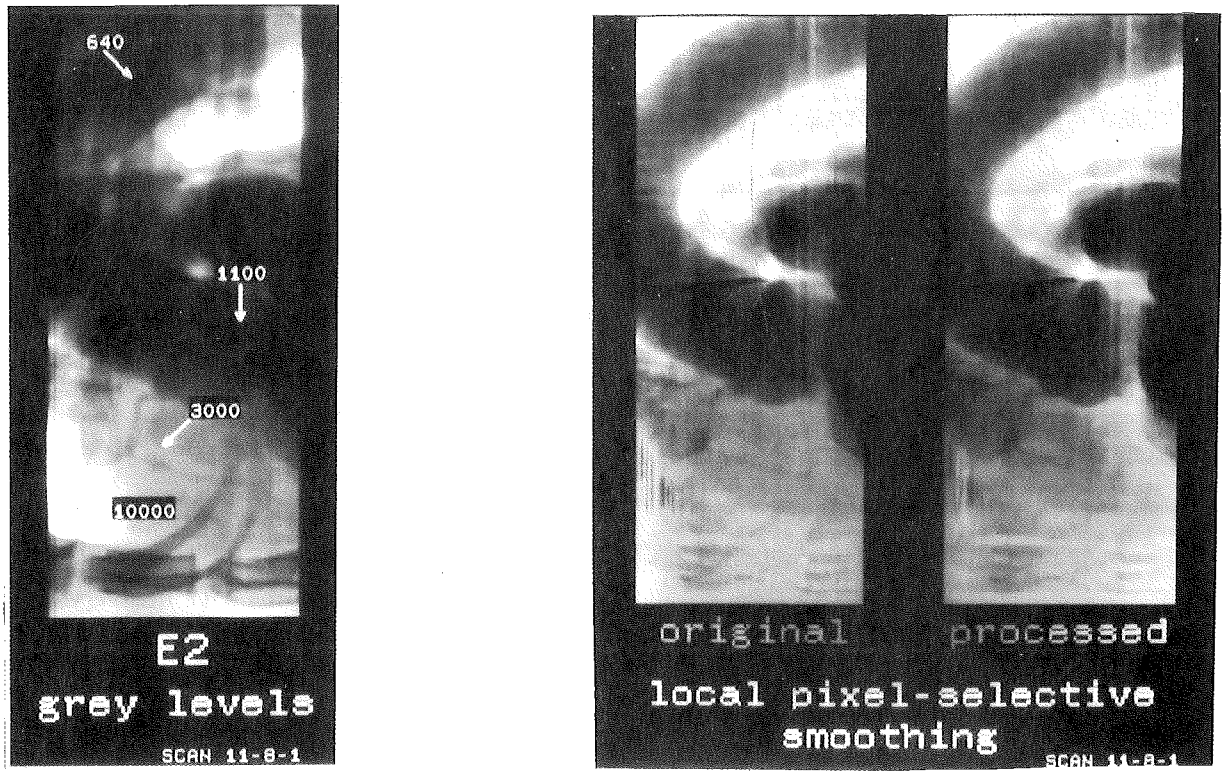

Figure 7: (a) Grey levels in different parts of the energy image (E_2). (b) Result of an image processing algorithm (edge preserving smoothing).

• To remove fixed pattern, each column x_i is adjusted relative to column x_{i-1}, starting at column 2.

The result of these procedures is shown in Figs.6a and 6b. The two images are shifted vertically according to the distance of the two beams in the dog and horizontally according to the divergence of the two beams. After division of the two images ($p_{i,j} = p_{2,i,j}/p_{1,i,j}$) the following corrections to the resulting subtraction image are carried out:
• The column normalization is repeated.
• The same procedure is used for line normalization.
• After cutting off 3% of the highest and 1% of the lowest grey values the minimum value is set to 0 and the maximum value is set to 250.
• After selecting a window in the image the grey level adjustment procedure is repeated.

In the resulting image (Fig.6c) part of the catheter, positioned in the vena cava superior, superposes the aorta in the left part of the image. Vena cava, right heart chambers and pulmonary arteries are free of contrast medium. Left chambers and aorta are filled with iodine and clearly visible. The right coronary artery shows up in the bottom part of the image (marked with arrows). The iodine structures left of the right coronary artery are due to a contrast depot in the vena cava. The root of the left coronary arteries is hardly visible because of superposition by the left chambers. This demonstrates the importance of finding projection angles for investigations of patients at which the small arteries are not superposed by large iodinated structures[10]. Furthermore the image shows that problems with the subtraction arise for those parts where the grey levels are extremely high (lung tissue) or low (iodine structure superposed by ribs) (see Fig.7a). Therefore the dynamic range of the detector must be further increased. Nevertheless the images from NIKOS II clearly show more contrast than those from NIKOS I. The SNR of the $1.5mm$ artery is 4 compared to 2 of a $1mm$ structure in the old system. Further improvements are expected by using the proposed image processing algorithms[11] and by correcting for the crosstalk and afterglow in the detector. A preliminary example is shown in Fig.7b.

5. OUTLOOK

The performance of the system NIKOS II now has reached a level at which the investigation of patients can be prepared. For this purpose the intensity of the monochromatic beams must be increased by at least a factor of 2 because of the larger thickness of the human thorax compared to that of the investigated dogs. Assuming a scan speed of $50cm/s$ in the final system (compared to $12.5cm/s$ during the present investigations) the photon flux in NIKOS II must be improved by a total factor of 8.

For the investigations of patients it is essential that the beam width at the patient is $12.5cm$ to cover the heart. This implies that the monochromator under development (2 bent crystals in Laue case) is installed and that the new glass fiber optics is included in the detector. With the new monochromator the intensity of the monochromatic beams is increased by a factor of about 10, giving the factor for the needed improvement of NIKOS II. The improvement of the wiggler HARWI with the help of a variable vacuum chamber is a long-term project. Further improvements can be achieved by increasing the dynamic range through modifications of the electronics und a higher gain due to the image intensifiers. This should increase the SNR in the images.

For the investigation of patients, planned in 1989, the special chair must be mounted on the scanning device and the safety system must be installed and incorporated in the general DESY safety system. These two projects are underway.

6. ACKNOWLEDGEMENTS

We thank the Werner-Otto-Stiftung for financial support. The authors would like to thank Mrs. Reusch for assistance in preparing the dogs for the investigations and the Dept. of Veterinary Medicine (Dir: Dr.med.vet. Dimigen).

7. REFERENCES

1. E. Rubenstein, R. Hofstadter, H.D. Zeman, A.C. Thompson, J.N. Otis, G.S. Brown, J.C. Giacomini, H.J. Gordon, R.S. Kernoff, D.C. Harrison, W.Thomlinson, "Transvenous coronary angiography in humans using synchrotron radiation", Proc. Natl. Acad. Sci. USA 83, 9724 (1986).

2. A. Akisada, M. Ando, K. Hyodo, S. Hasegawa, K. Konishi, K. Nishimura, A. Maruhashi, F. Toyofuku, A. Suwa, K. Kohra, "An Attempt at Coronary Angiography with a Large Size Monochromatic SR Beam", NIM A246, 713 (1986).

3. W.-R. Dix, K. Engelke, C.-C. Glüer, W. Graeff, H. Jabs, W. Kupper, K.-H. Stellmaschek, "NIKOS - a system for non-invasive examination of coronary arteries by means of DSA with synchrotron radiation", IEEE Computer Society 817, 73 (1987).

4. W. Graeff, W.-R. Dix, "NIKOS - non-invasive angiography at HASYLAB", in Synchrotron Radiation Handbook, Vol.4 (in preparation).

5. L.T. Niklason, J.A. Sorenson, J.A. Nelson, "Scattered Radiation in Chest Radiography", Med.Phys. 8, 677 (1981).

6. W. Graeff, L. Bittner, W. Brefeld, U. Hahn, G. Heintze, J. Heuer, J. Kouptsidis, J. Pflüger, M. Schwartz, E.W. Weiner, T. Wroblewski, "HARWI a Hard X-Ray Wiggler Beam at DORIS", Rev.Sci.Instr. (accepted for publication).

7. W. Graeff, W.-R. Dix, W. Kupper, "An Overview of Different Technical Approaches to SYRDA", in Synchrotron Radiation Applications to Digital Subtraction Angiography (SYRDA), E. Burattini, A. Rindi, eds., Italian Physical Society, Proc. Vol. 10, 45 (1988).

8. P. Suortti, W. Thomlinson, "A bent Laue crystal monochromator for angiography at the NSLS", NIM A269, 639 (1988).

9. C.-C. Glüer, K. Engelke, W.-R. Dix, W. Graeff, W. Kupper, K.-H. Stellmaschek, "A fast low-noise line scan X-ray detector", Med.Phys. 16, 98 (1989).

10. W. Kupper, W.-R. Dix, W. Graeff, P. Steiner, K. Engelke, C.-C. Glüer, W. Bleifeld, "Projection Angles for Intravenous Coronary Angiography", in Synchrotron Radiation Applications to Digital Subtraction Angiography (SYRDA), E. Burattini, A. Rindi, eds., Italian Physical Society, Proc. Vol. 10, 165 (1988).

11. W.-R. Dix, W. Graeff, W. Kupper, "Image Processing of SYRDA Pictures", in Synchrotron Radiation Applications to Digital Subtraction Angiography (SYRDA), E. Burattini, A. Rindi, eds., Italian Physical Society, Proc. Vol. 10, 95 (1988).